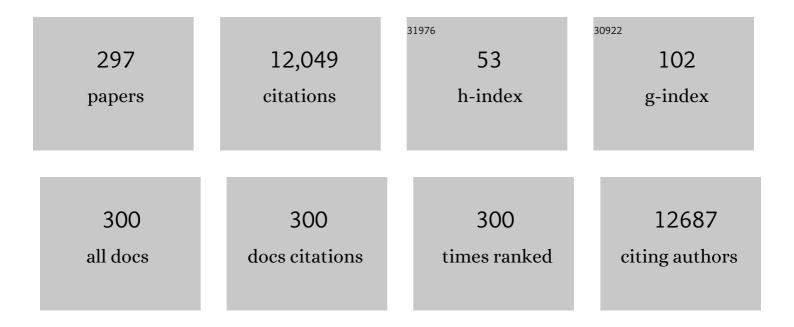
Tian-Ling Ren

List of Publications by Year in descending order

Source: https://exaly.com/author-pdf/4283062/publications.pdf Version: 2024-02-01



#	Article	IF	CITATIONS
1	Carbonized Silk Fabric for Ultrastretchable, Highly Sensitive, and Wearable Strain Sensors. Advanced Materials, 2016, 28, 6640-6648.	21.0	749
2	Epidermis Microstructure Inspired Graphene Pressure Sensor with Random Distributed Spinosum for High Sensitivity and Large Linearity. ACS Nano, 2018, 12, 2346-2354.	14.6	579
3	Graphene-Paper Pressure Sensor for Detecting Human Motions. ACS Nano, 2017, 11, 8790-8795.	14.6	572
4	Graphene Textile Strain Sensor with Negative Resistance Variation for Human Motion Detection. ACS Nano, 2018, 12, 9134-9141.	14.6	455
5	A Graphene-Based Resistive Pressure Sensor with Record-High Sensitivity in a Wide Pressure Range. Scientific Reports, 2015, 5, 8603.	3.3	415
6	An intelligent artificial throat with sound-sensing ability based on laser induced graphene. Nature Communications, 2017, 8, 14579.	12.8	396
7	Flexible, Highly Sensitive, and Wearable Pressure and Strain Sensors with Graphene Porous Network Structure. ACS Applied Materials & Interfaces, 2016, 8, 26458-26462.	8.0	387
8	Scalable fabrication of high-performance and flexible graphene strain sensors. Nanoscale, 2014, 6, 699-705.	5.6	366
9	Extremely Low Operating Current Resistive Memory Based on Exfoliated 2D Perovskite Single Crystals for Neuromorphic Computing. ACS Nano, 2017, 11, 12247-12256.	14.6	286
10	Wearable humidity sensor based on porous graphene network for respiration monitoring. Biosensors and Bioelectronics, 2018, 116, 123-129.	10.1	278
11	Multilayer Graphene Epidermal Electronic Skin. ACS Nano, 2018, 12, 8839-8846.	14.6	257
12	Vertical MoS2 transistors with sub-1-nm gate lengths. Nature, 2022, 603, 259-264.	27.8	251
13	Graphene Dynamic Synapse with Modulatable Plasticity. Nano Letters, 2015, 15, 8013-8019.	9.1	226
14	Graphene-on-Paper Sound Source Devices. ACS Nano, 2011, 5, 4878-4885.	14.6	197
15	Triode-Mimicking Graphene Pressure Sensor with Positive Resistance Variation for Physiology and Motion Monitoring. ACS Nano, 2020, 14, 10104-10114.	14.6	180
16	Graphene/semiconductor heterojunction solar cells with modulated antireflection and graphene work function. Energy and Environmental Science, 2013, 6, 108-115.	30.8	154
17	Novel Field-Effect Schottky Barrier Transistors Based on Graphene-MoS2 Heterojunctions. Scientific Reports, 2014, 4, 5951.	3.3	134
18	Photoelectric Synaptic Plasticity Realized by 2D Perovskite. Advanced Functional Materials, 2019, 29, 1902538.	14.9	132

#	Article	IF	CITATIONS
19	Monitoring Oxygen Movement by Raman Spectroscopy of Resistive Random Access Memory with a Graphene-Inserted Electrode. Nano Letters, 2013, 13, 651-657.	9.1	121
20	Simultaneously Detecting Subtle and Intensive Human Motions Based on a Silver Nanoparticles Bridged Graphene Strain Sensor. ACS Applied Materials & Interfaces, 2018, 10, 3948-3954.	8.0	118
21	Cost-Effective, Transfer-Free, Flexible Resistive Random Access Memory Using Laser-Scribed Reduced Graphene Oxide Patterning Technology. Nano Letters, 2014, 14, 3214-3219.	9.1	114
22	A spectrally tunable all-graphene-based flexible field-effect light-emitting device. Nature Communications, 2015, 6, 7767.	12.8	113
23	Wafer-Scale Integration of Graphene-based Electronic, Optoelectronic and Electroacoustic Devices. Scientific Reports, 2014, 4, 3598.	3.3	113
24	Multifunctional Graphene Microstructures Inspired by Honeycomb for Ultrahigh Performance Electromagnetic Interference Shielding and Wearable Applications. ACS Nano, 2021, 15, 8907-8918.	14.6	110
25	High performance flexible strain sensor based on self-locked overlapping graphene sheets. Nanoscale, 2016, 8, 20090-20095.	5.6	108
26	Graphene Earphones: Entertainment for Both Humans and Animals. ACS Nano, 2014, 8, 5883-5890.	14.6	105
27	Ultra-High Sensitive NO ₂ Gas Sensor Based on Tunable Polarity Transport in CVD-WS ₂ /IGZO p-N Heterojunction. ACS Applied Materials & Interfaces, 2019, 11, 40850-40859.	8.0	105
28	Self-adapted and tunable graphene strain sensors for detecting both subtle and large human motions. Nanoscale, 2017, 9, 8266-8273.	5.6	100
29	Graphene-based wearable sensors. Nanoscale, 2019, 11, 18923-18945.	5.6	98
30	Enhanced photovoltaic properties in graphene/polycrystalline BiFeO3/Pt heterojunction structure. Applied Physics Letters, 2011, 99, .	3.3	97
31	Wearable Electronics Based on 2D Materials for Human Physiological Information Detection. Small, 2020, 16, e1901124.	10.0	97
32	A miniaturized microbial fuel cell with three-dimensional graphene macroporous scaffold anode demonstrating a record power density of over 10 000 W m ^{â^'3} . Nanoscale, 2016, 8, 3539-3547.	5.6	96
33	Simultaneous synthesis and integration of two-dimensional electronic components. Nature Electronics, 2019, 2, 164-170.	26.0	95
34	Single-layer graphene sound-emitting devices: experiments and modeling. Nanoscale, 2012, 4, 2272.	5.6	92
35	High-performance graphene-based flexible heater for wearable applications. RSC Advances, 2017, 7, 27001-27006.	3.6	91
36	Ultrafast Photodetector by Integrating Perovskite Directly on Silicon Wafer. ACS Nano, 2020, 14, 2860-2868.	14.6	86

#	Article	IF	CITATIONS
37	A Wearable Skinlike Ultra-Sensitive Artificial Graphene Throat. ACS Nano, 2019, 13, 8639-8647.	14.6	80
38	An ultrasensitive strain sensor with a wide strain range based on graphene armour scales. Nanoscale, 2018, 10, 11524-11530.	5.6	77
39	Graphene based Schottky junction solar cells on patterned silicon-pillar-array substrate. Applied Physics Letters, 2011, 99, 233505.	3.3	76
40	A Pressure Sensing System for Heart Rate Monitoring with Polymer-Based Pressure Sensors and An Anti-Interference Post Processing Circuit. Sensors, 2015, 15, 3224-3235.	3.8	76
41	Heterostructured graphene quantum dot/WSe2/Si photodetector with suppressed dark current and improved detectivity. Nano Research, 2018, 11, 3233-3243.	10.4	67
42	Multifunctional and high-performance electronic skin based on silver nanowires bridging graphene. Carbon, 2020, 156, 253-260.	10.3	67
43	A Better Zn-Ion Storage Device: Recent Progress for Zn-Ion Hybrid Supercapacitors. Nano-Micro Letters, 2022, 14, 64.	27.0	65
44	A super flexible and custom-shaped graphene heater. Nanoscale, 2017, 9, 14357-14363.	5.6	63
45	Two-stage amplification of an ultrasensitive MXene-based intelligent artificial eardrum. Science Advances, 2022, 8, eabn2156.	10.3	62
46	Observation of a giant two-dimensional band-piezoelectric effect on biaxial-strained graphene. NPG Asia Materials, 2015, 7, e154-e154.	7.9	58
47	X-Ray Detector Based on All-Inorganic Lead-Free Cs ₂ AgBiBr ₆ Perovskite Single Crystal. IEEE Transactions on Electron Devices, 2019, 66, 2224-2229.	3.0	57
48	Graphene-Based Multifunctional Textile for Sensing and Actuating. ACS Nano, 2021, 15, 17738-17747.	14.6	57
49	Transparent, flexible, ultrathin sound source devices using Indium Tin oxide films. Applied Physics Letters, 2011, 99, .	3.3	56
50	Growth and Raman Spectra of Single-Crystal Trilayer Graphene with Different Stacking Orientations. ACS Nano, 2014, 8, 10766-10773.	14.6	56
51	Enhanced dielectric and multiferroic properties of single-phase Y and Zr co-doped BiFeO3 ceramics. Journal of Applied Physics, 2013, 114, .	2.5	55
52	Flexible CNT-array double helices Strain Sensor with high stretchability for Motion Capture. Scientific Reports, 2015, 5, 15554.	3.3	55
53	In Situ Tuning of Switching Window in a Gate ontrolled Bilayer Grapheneâ€Electrode Resistive Memory Device. Advanced Materials, 2015, 27, 7767-7774.	21.0	54
54	All-Inorganic Perovskite Nanowires–InGaZnO Heterojunction for High-Performance Ultraviolet–Visible Photodetectors. ACS Applied Materials & Interfaces, 2018, 10, 7231-7238.	8.0	53

#	Article	IF	CITATIONS
55	Flexible Two-Dimensional Ti ₃ C ₂ MXene Films as Thermoacoustic Devices. ACS Nano, 2019, 13, 12613-12620.	14.6	53
56	Interface Engineering with MoS ₂ –Pd Nanoparticles Hybrid Structure for a Low Voltage Resistive Switching Memory. Small, 2018, 14, 1702525.	10.0	52
57	Controllable Thermal Rectification Realized in Binary Phase Change Composites. Scientific Reports, 2015, 5, 8884.	3.3	49
58	A Review on Bacteriorhodopsin-Based Bioelectronic Devices. Sensors, 2018, 18, 1368.	3.8	47
59	Flexible, ultrathin, and transparent sound-emitting devices using silver nanowires film. Applied Physics Letters, 2011, 99, .	3.3	46
60	A high performance triboelectric nanogenerator for self-powered non-volatile ferroelectric transistor memory. Nanoscale, 2015, 7, 17306-17311.	5.6	46
61	Graphene FET Array Biosensor Based on ssDNA Aptamer for Ultrasensitive Hg2+ Detection in Environmental Pollutants. Frontiers in Chemistry, 2018, 6, 333.	3.6	46
62	Light-Enhanced Ion Migration in Two-Dimensional Perovskite Single Crystals Revealed in Carbon Nanotubes/Two-Dimensional Perovskite Heterostructure and Its Photomemory Application. ACS Central Science, 2019, 5, 1857-1865.	11.3	45
63	Electrooculography and Tactile Perception Collaborative Interface for 3D Human–Machine Interaction. ACS Nano, 2022, 16, 6687-6699.	14.6	44
64	Long-Term Depression Mimicked in an IGZO-Based Synaptic Transistor. IEEE Electron Device Letters, 2017, 38, 191-194.	3.9	43
65	A Ferroelectric Thin Film Transistor Based on Annealing-Free HfZrO Film. IEEE Journal of the Electron Devices Society, 2017, 5, 378-383.	2.1	43
66	Substrate-Free Multilayer Graphene Electronic Skin for Intelligent Diagnosis. ACS Applied Materials & Interfaces, 2020, 12, 49945-49956.	8.0	43
67	Switching dynamics of ferroelectric HfO2-ZrO2 with various ZrO2 contents. Applied Physics Letters, 2019, 114, .	3.3	42
68	Intelligent and Multifunctional Graphene Nanomesh Electronic Skin with High Comfort. Small, 2022, 18, e2104810.	10.0	42
69	Encapsulated X-Ray Detector Enabled by All-Inorganic Lead-Free Perovskite Film With High Sensitivity and Low Detection Limit. IEEE Transactions on Electron Devices, 2020, 67, 3191-3198.	3.0	40
70	Highly Transparent and Sensitive Graphene Sensors for Continuous and Non-invasive Intraocular Pressure Monitoring. ACS Applied Materials & Interfaces, 2020, 12, 18375-18384.	8.0	40
71	A flexible, transparent and ultrathin single-layer graphene earphone. RSC Advances, 2015, 5, 17366-17371.	3.6	39
72	Tunable graphene oxide reduction and graphene patterning at room temperature on arbitrary substrates. Carbon, 2016, 109, 173-181.	10.3	38

#	Article	IF	CITATIONS
73	Influence of La and Mn dopants on the current-voltage characteristics of BiFeO3/ZnO heterojunction. Journal of Applied Physics, 2012, 111, .	2.5	37
74	The Trend of 2D Transistors toward Integrated Circuits: Scaling Down and New Mechanisms. Advanced Materials, 2022, 34, e2201916.	21.0	37
75	Temperature Control of P(VDF-TrFE) Copolymer Thin Films. Integrated Ferroelectrics, 2013, 141, 187-194.	0.7	36
76	Efficient and Reversible Electron Doping of Semiconductor-Enriched Single-Walled Carbon Nanotubes by Using Decamethylcobaltocene. Scientific Reports, 2017, 7, 6751.	3.3	36
77	Locally hydrazine doped WSe ₂ p-n junction toward high-performance photodetectors. Nanotechnology, 2018, 29, 015203.	2.6	36
78	Multifunctional Mechanical Sensors for Versatile Physiological Signal Detection. ACS Applied Materials & amp; Interfaces, 2018, 10, 44173-44182.	8.0	36
79	High-Quality Single Crystal Perovskite for Highly Sensitive X-Ray Detector. IEEE Electron Device Letters, 2020, 41, 256-259.	3.9	36
80	Selfâ€Powered MoS ₂ –PDPP3T Heterotransistorâ€Based Broadband Photodetectors. Advanced Electronic Materials, 2019, 5, 1800580.	5.1	35
81	Ferroelectric structural transition in hafnium oxide induced by charged oxygen vacancies. Physical Review B, 2021, 104, .	3.2	35
82	Review on Organic–Inorganic Two-Dimensional Perovskite-Based Optoelectronic Devices. ACS Applied Electronic Materials, 2022, 4, 547-567.	4.3	35
83	Ultra-sensitive and plasmon-tunable graphene photodetectors for micro-spectrometry. Nanoscale, 2018, 10, 20013-20019.	5.6	34
84	Coherent Generation of Photo-Thermo-Acoustic Wave from Graphene Sheets. Scientific Reports, 2015, 5, 10582.	3.3	33
85	Graphene-Based Thermoacoustic Sound Source. ACS Nano, 2020, 14, 3779-3804.	14.6	33
86	Top-Gate Electric-Double-Layer IZO-Based Synaptic Transistors for Neuron Networks. IEEE Electron Device Letters, 2017, 38, 588-591.	3.9	32
87	Flexible Quasiâ€van der Waals Ferroelectric Hafniumâ€Based Oxide for Integrated Highâ€Performance Nonvolatile Memory. Advanced Science, 2020, 7, 2001266.	11.2	32
88	Resistive switching behavior in diamond-like carbon films grown by pulsed laser deposition for resistance switching random access memory application. Journal of Applied Physics, 2012, 111, 084501.	2.5	31
89	Stable InSe transistors with high-field effect mobility for reliable nerve signal sensing. Npj 2D Materials and Applications, 2019, 3, .	7.9	31
90	Compact, Flexible, and Transparent Antennas Based on Embedded Metallic Mesh for Wearable Devices in 5G Wireless Network. IEEE Transactions on Antennas and Propagation, 2021, 69, 1864-1873.	5.1	31

#	Article	IF	CITATIONS
91	Grapheneâ€Based Devices for Thermal Energy Conversion and Utilization. Advanced Functional Materials, 2020, 30, 1903888.	14.9	30
92	Controlled Growth of Bilayerâ€MoS ₂ Films and MoS ₂ â€Based Fieldâ€Effect Transistor (FET) Performance Optimization. Advanced Electronic Materials, 2018, 4, 1700524.	5.1	29
93	A contact lens promising for non-invasive continuous intraocular pressure monitoring. RSC Advances, 2019, 9, 5076-5082.	3.6	29
94	Static behavior of a graphene-based sound-emitting device. Nanoscale, 2012, 4, 3345.	5.6	28
95	Fabrication and Characterization of a Novel Si Line Tunneling TFET With High Drive Current. IEEE Journal of the Electron Devices Society, 2020, 8, 336-340.	2.1	28
96	High-performance single crystal CH3NH3PbI3 perovskite x-ray detector. Applied Physics Letters, 2021, 118, .	3.3	28
97	Piezoelectric and ferroelectric films for microelectronic applications. Materials Science and Engineering B: Solid-State Materials for Advanced Technology, 2003, 99, 159-163.	3.5	27
98	Fabricating Molybdenum Disulfide Memristors. ACS Applied Electronic Materials, 2020, 2, 346-370.	4.3	27
99	Negative Capacitance Oxide Thin-Film Transistor With Sub-60 mV/Decade Subthreshold Swing. IEEE Electron Device Letters, 2019, 40, 826-829.	3.9	26
100	Large-Scale and High-Density pMUT Array Based on Isolated Sol-Gel PZT Membranes for Fingerprint Imaging. Journal of the Electrochemical Society, 2017, 164, B377-B381.	2.9	25
101	Wafer-Scale Photolithography-Pixeled Pb-Free Perovskite X-ray Detectors. ACS Nano, 2022, 16, 10199-10208.	14.6	25
102	Poly(3,4-ethylenedioxythiophene):poly(styrenesulfonate)-based organic, ultrathin, and transparent sound-emitting device. Applied Physics Letters, 2011, 99, 233503.	3.3	24
103	Flexible graphene sound device based on laser reduced graphene. Applied Physics Letters, 2017, 111, .	3.3	24
104	Proton Conductor Gated Synaptic Transistor Based on Transparent IGZO for Realizing Electrical and UV Light Stimulus. IEEE Journal of the Electron Devices Society, 2019, 7, 38-45.	2.1	24
105	A novel MEMS pressure sensor with MOSFET on chip. , 2008, , .		23
106	Investigation of the improved performance in a graphene/polycrystalline BiFeO3/Pt photovoltaic heterojunction: Experiment, modeling, and application. Journal of Applied Physics, 2012, 112, .	2.5	23
107	A reduced graphene oxide sound-emitting device: a new use for Joule heating. RSC Advances, 2013, 3, 17672.	3.6	22
108	Two-Mode MoS ₂ Filament Transistor with Extremely Low Subthreshold Swing and Record High On/Off Ratio. ACS Nano, 2019, 13, 2205-2212.	14.6	22

#	Article	IF	CITATIONS
109	An efficient flexible graphene-based light-emitting device. Nanoscale Advances, 2019, 1, 4745-4754.	4.6	22
110	Observation of negative capacitance in antiferroelectric PbZrO3 Films. Nature Communications, 2021, 12, 4215.	12.8	22
111	Black phosphorus junctions and their electrical and optoelectronic applications. Journal of Semiconductors, 2021, 42, 081001.	3.7	22
112	Ultrasensitive Detection of COVID-19 Causative Virus (SARS-CoV-2) Spike Protein Using Laser Induced Graphene Field-Effect Transistor. Molecules, 2021, 26, 6947.	3.8	22
113	Humidity-Based Human–Machine Interaction System for Healthcare Applications. ACS Applied Materials & Interfaces, 2022, 14, 12606-12616.	8.0	22
114	Hybrid graphene/cadmium-free ZnSe/ZnS quantum dots phototransistors for UV detection. Scientific Reports, 2018, 8, 5107.	3.3	21
115	A Grapheneâ€Based Filament Transistor with Subâ€10 mVdec ^{â^'1} Subthreshold Swing. Advanced Electronic Materials, 2018, 4, 1700608.	5.1	21
116	High Performance 2D Perovskite/Graphene Optical Synapses as Artificial Eyes. , 2018, , .		21
117	Gate-Tunable Negative Differential Resistance Behaviors in a hBN-Encapsulated BP-MoS ₂ Heterojunction. ACS Applied Materials & Interfaces, 2021, 13, 26161-26169.	8.0	21
118	An Integrated Luminescent Information Encryption–Decryption and Anticounterfeiting Chip Based on Laser Induced Graphene. Advanced Functional Materials, 2021, 31, 2103255.	14.9	21
119	Structural, ferroelectric, dielectric, and magnetic properties of BiFeO3/Bi3.15Nd0.85Ti3O12 multilayer films derived by chemical solution deposition. Journal of Applied Physics, 2009, 105, 084109.	2.5	20
120	Highly Sensitive, Wide-Range, and Flexible Pressure Sensor Based on Honeycomb-Like Graphene Network. IEEE Transactions on Electron Devices, 2020, 67, 2153-2156.	3.0	20
121	Graphene devices based on laser scribing technology. Japanese Journal of Applied Physics, 2018, 57, 04FA01.	1.5	19
122	A Flexible 360-Degree Thermal Sound Source Based on Laser Induced Graphene. Nanomaterials, 2016, 6, 112.	4.1	18
123	Au Nanoparticles-Decorated Surface Plasmon Enhanced ZnO Nanorods Ultraviolet Photodetector on Flexible Transparent Mica Substrate. IEEE Journal of the Electron Devices Society, 2019, 7, 196-202.	2.1	18
124	Unipolar to ambipolar conversion in graphene field-effect transistors. Applied Physics Letters, 2012, 101, .	3.3	17
125	Wearable Strain Sensors: Carbonized Silk Fabric for Ultrastretchable, Highly Sensitive, and Wearable Strain Sensors (Adv. Mater. 31/2016). Advanced Materials, 2016, 28, 6639-6639.	21.0	17
126	A Miniaturized Integrated SAW Sensing System for Relative Humidity Based on Graphene Oxide Film. IEEE Sensors Journal, 2020, 20, 9733-9739.	4.7	16

#	Article	IF	CITATIONS
127	Effects of anode materials on resistive characteristics of NiO thin films. Applied Physics Letters, 2013, 102, .	3.3	15
128	A Low Input Current and Wide Conversion Ratio Buck Regulator with 75% Efficiency for High-Voltage Triboelectric Nanogenerators. Scientific Reports, 2016, 6, 19246.	3.3	15
129	High performance photodetector based on Pd-single layer MoS2 Schottky junction. Applied Physics Letters, 2016, 109, .	3.3	15
130	A point acoustic device based on aluminum nanowires. Nanoscale, 2016, 8, 5516-5525.	5.6	15
131	Synaptic Computation Demonstrated in a Two-Synapse Network Based on Top-Gate Electric-Double-Layer Synaptic Transistors. IEEE Electron Device Letters, 2017, 38, 1496-1499.	3.9	15
132	Design and Characterization of High-Density Ultrasonic Transducer Array. IEEE Sensors Journal, 2018, 18, 2285-2290.	4.7	15
133	Negative Capacitance Black Phosphorus Transistors With Low SS. IEEE Transactions on Electron Devices, 2019, 66, 1579-1583.	3.0	15
134	Highly stretchable and conformal electromagnetic interference shielding armor with strain sensing ability. Chemical Engineering Journal, 2022, 431, 133908.	12.7	15
135	Highâ€Throughput DNA Tensioner Platform for Interrogating Mechanical Heterogeneity of Single Living Cells. Small, 2022, 18, e2106196.	10.0	15
136	Surface acoustic wave characteristics based on c-axis (006) LiNbO3/diamond/silicon layered structure. Applied Physics Letters, 2011, 99, .	3.3	14
137	Millimeter-Scale Nonlocal Photo-Sensing Based on Single-Crystal Perovskite Photodetector. IScience, 2018, 7, 110-119.	4.1	14
138	A Hybrid Phototransistor Neuromorphic Synapse. IEEE Journal of the Electron Devices Society, 2019, 7, 13-17.	2.1	14
139	An intelligent nanomesh-reinforced graphene pressure sensor with an ultra large linear range. Journal of Materials Chemistry A, 2022, 10, 4858-4869.	10.3	14
140	Characterization of Pt/Bi3.15Nd0.85Ti3O12/HfO2/Si structure using a hafnium oxide as buffer layer for ferroelectric-gate field effect transistors. Journal of Applied Physics, 2009, 106, .	2.5	13
141	Characteristics of Pt/BiFeO3/TiO2/Si capacitors with TiO2 layer formed by liquid-delivery metal organic chemical vapor deposition. Applied Physics Letters, 2010, 97, .	3.3	13
142	MoS ₂ Synaptic Transistor With Tunable Weight Profile. IEEE Transactions on Electron Devices, 2018, 65, 3543-3547.	3.0	13
143	Plasmonâ€Enhanced InGaZnO Ultraviolet Photodetectors Tuned by Ferroelectric HfZrO. Advanced Electronic Materials, 2019, 5, 1900588.	5.1	13
144	Laser-reconfigured MoS2/ZnO van der Waals synapse. Nanoscale, 2019, 11, 11114-11120.	5.6	13

#	Article	IF	CITATIONS
145	Development of a portable setup using a miniaturized and high precision colorimeter for the estimation of phosphate in natural water. Analytica Chimica Acta, 2019, 1058, 70-79.	5.4	13
146	Programmable Sensitivity Screening of Strain Sensors by Local Electrical and Mechanical Properties Coupling. ACS Nano, 2021, 15, 20590-20599.	14.6	13
147	Nomex paper-based double-sided laser-induced graphene for multifunctional human-machine interfaces. Carbon, 2022, 193, 68-76.	10.3	13
148	Electrode/oxide interface engineering by inserting single-layer graphene: Application for HfO <inf>x</inf> -based resistive random access memory. , 2012, , .		12
149	High-performance sound source devices based on graphene woven fabrics. Applied Physics Letters, 2017, 110, .	3.3	12
150	The Origin of CBRAM With High Linearity, On/Off Ratio, and State Number for Neuromorphic Computing. IEEE Transactions on Electron Devices, 2021, 68, 2568-2571.	3.0	12
151	Graphene-Based Flexible Electrode for Electrocardiogram Signal Monitoring. Applied Sciences (Switzerland), 2022, 12, 4526.	2.5	12
152	Ultrasonic transducer array design for medical imaging based on MEMS technologies. , 2010, , .		11
153	Toward an In Situ Phosphate Sensor in Natural Waters Using a Microfluidic Flow Loop Analyzer. Journal of the Electrochemical Society, 2018, 165, B737-B745.	2.9	11
154	Field effect properties of single-layer MoS2(1â^'x)Se2x nanosheets produced by a one-step CVD process. Journal of Materials Science, 2018, 53, 14447-14455.	3.7	11
155	Electromyogram-strain synergetic intelligent artificial throat. Chemical Engineering Journal, 2022, 449, 137741.	12.7	11
156	Ambipolar/unipolar conversion in graphene transistors by surface doping. Applied Physics Letters, 2013, 103, 193502.	3.3	10
157	A novel cell-scale bio-nanogenerator based on electron–ion interaction for fast light power conversion. Nanoscale, 2018, 10, 526-532.	5.6	10
158	A novel thermal acoustic device based on vertical graphene film. AIP Advances, 2019, 9, 075302.	1.3	10
159	A Shoe-Integrated Sensor System for Long- Term Center of Pressure Evaluation. IEEE Sensors Journal, 2021, 21, 27037-27044.	4.7	10
160	Filling the gap: thermal properties and device applications of graphene. Science China Information Sciences, 2021, 64, 1.	4.3	10
161	Reconfigurable Logic-Memory Hybrid Device Based on Ferroelectric Hf _{0.5} Zr _{0.5} O ₂ . IEEE Electron Device Letters, 2021, 42, 1164-1167.	3.9	10
162	Ultrathin encapsulated rGO strain sensor for gesture recognition. Microelectronic Engineering, 2022, 259, 111779.	2.4	10

#	Article	IF	CITATIONS
163	A novel ferroelectric based microphone. Microelectronic Engineering, 2003, 66, 683-687.	2.4	9
164	A novel thermal acoustic device based on porous graphene. AIP Advances, 2016, 6, .	1.3	9
165	Lower Power, Better Uniformity, and Stability CBRAM Enabled by Graphene Nanohole Interface Engineering. IEEE Transactions on Electron Devices, 2020, 67, 984-988.	3.0	9
166	Reconfigurable MoTe ₂ Field-Effect Transistors and its Application in Compact CMOS Circuits. IEEE Transactions on Electron Devices, 2021, 68, 4748-4753.	3.0	9
167	A 10Ânm Short Channel MoS ₂ Transistor without the Resolution Requirement of Photolithography. Advanced Electronic Materials, 2021, 7, 2100543.	5.1	9
168	NOVEL DEVICE DESIGN FOR AN ULTRASONIC RANGING SYSTEM. Integrated Ferroelectrics, 2009, 105, 53-65.	0.7	8
169	Demonstration of α-InGaZnO TFT Nonvolatile Memory Using TiAlO Charge Trapping Layer. IEEE Nanotechnology Magazine, 2018, 17, 1089-1093.	2.0	8
170	Roll-to-roll graphene films for non-disposable electrocardiogram electrodes. Journal Physics D: Applied Physics, 2021, 54, 364003.	2.8	8
171	Impact of Molybdenum Oxide Electrode on the Ferroelectricity of Doped-Hafnia Oxide Capacitors. IEEE Transactions on Electron Devices, 2022, 69, 1492-1496.	3.0	8
172	DEVICE DESIGN FOR THE NOVEL HANDWRITING RECOGNITION SYSTEM. Integrated Ferroelectrics, 2008, 100, 206-215.	0.7	7
173	Design of magnetic RF inductor in CMOS. Tsinghua Science and Technology, 2012, 17, 78-83.	6.1	7
174	Surface Acoustic Wave Devices Based on High Quality Temperature-Compensated Substrates. IEEE Electron Device Letters, 2016, 37, 1063-1066.	3.9	7
175	Low-Voltage Unipolar Inverter Based on Top-Gate Electric-Double-Layer Thin-Film Transistors Gated by Silica Proton Conductor. IEEE Electron Device Letters, 2017, 38, 875-878.	3.9	7
176	Fabrication and Properties of \$hbox{Pt}/hbox{Bi}_{3.15}hbox{Nd}_{0.85} hbox{Ti}_{3}hbox{O}_{12}/reakhbox{HfO}_{2}/hbox{Si}\$ Structure for Ferroelectric DRAM (FEDRAM) FET. IEEE Electron Device Letters, 2009, 30, 463-465.	3.9	6
177	Comparative Study on Structural and Ferroelectric Properties of Dual-Site Rare-Earth lons Substituted Multiferroelectric BiFeO ₃ . Integrated Ferroelectrics, 2012, 132, 30-38.	0.7	6
178	Temperature dependence of optical and structural properties of ferroelectric B3.15Nd0.85Ti3O12 thin film derived by sol–gel process. Journal of Sol-Gel Science and Technology, 2012, 61, 236-242.	2.4	6
179	Magnetoresistive behavior and magnetization reversal of NiFe/Cu/CoFe/IrMn spin valve GMRs in nanoscale. International Journal of Minerals, Metallurgy and Materials, 2013, 20, 700-704.	4.9	6
180	Ink-injected dual-band antennas based on graphene flakes, carbon nanotubes and silver nanowires. RSC Advances, 2018, 8, 37534-37539.	3.6	6

#	Article	IF	CITATIONS
181	Gait Recognition Based on Graphene Porous Network Structure Pressure Sensors for Rehabilitation Therapy. , 2018, , .		6
182	Fabrication and Characterization of Ferroelectric HfZrO-based Synaptic Transistors with Multi-state Plasticity. , 2020, , .		6
183	Intelligent and highly sensitive strain sensor based on indium tin oxide micromesh with a high crack density. Nanoscale, 2022, 14, 4234-4243.	5.6	6
184	Skinâ€Mimicking, Stretchable Photodetector for Skin ustomized Ultraviolet Dosimetry. Advanced Materials Technologies, 2022, 7, .	5.8	6
185	Electrospun Nanofibers for Integrated Sensing, Storage, and Computing Applications. Applied Sciences (Switzerland), 2022, 12, 4370.	2.5	6
186	Light-Controlled Reconfigurable Optical Synapse Based on Carbon Nanotubes/2D Perovskite Heterostructure for Image Recognition. ACS Applied Materials & Interfaces, 2022, 14, 28221-28229.	8.0	6
187	UNIFORMITY IMPROVEMENT OF PZT BASED ULTRASONIC TRANSDUCER. Integrated Ferroelectrics, 2006, 80, 373-381.	0.7	5
188	AN INNOVATED PROCESS OF Pt/PbTiO3/PbZr0.3Ti0.7O3/PbTiO3/Pt INTEGRATED FERROELECTRIC CAPACITORS FOR FeRAM. Integrated Ferroelectrics, 2007, 89, 3-11.	0.7	5
189	Modulation Effect of Lead Zirconate Titanate for Zinc Oxide Channel Resistance in Ferroelectric Field Effect Transistor. Ferroelectrics, 2011, 421, 92-97.	0.6	5
190	Hippocampal Neurons' Alignment on Quartz Grooves and Parylene Cues on Quartz Substrate. Applied Sciences (Switzerland), 2021, 11, 275.	2.5	5
191	Deep Learning Enabled High-Performance Speech Command Recognition on Graphene Flexible Microphones. ACS Applied Electronic Materials, 2022, 4, 2306-2312.	4.3	5
192	Studies of a PT/PZT/PT sandwich structure for feram applications using sol-gel processing. Integrated Ferroelectrics, 2001, 39, 215-222.	0.7	4
193	Measurements of Ferroelectric MEMS Microphones. Integrated Ferroelectrics, 2005, 69, 417-429.	0.7	4
194	Light-Induced Modulation in Resistance Switching of Carbon Nanotube/BiFeO ₃ /Pt Heterostructure. Integrated Ferroelectrics, 2012, 134, 58-64.	0.7	4
195	Optimization of graphene/silicon heterojunction solar cells. , 2012, , .		4
196	Flexible and large-area sound-emitting device using reduced graphene oxide. , 2013, , .		4
197	A multi-mode complex bandpass filter with gm-assisted power optimization and I/Q calibration. , 2013, , .		4
198	Zno field-effect transistors with lead-zirconate-titanate ferroelectric gate. Materials Research Innovations, 2015, 19, S2-181-S2-184.	2.3	4

#	Article	IF	CITATIONS
199	Graphene based Wearable Sensors for Healthcare. , 2019, , .		4
200	Tunable electronic and optical properties of the WS ₂ /IGZO heterostructure <i>via</i> an external electric field and strain: a theoretical study. Physical Chemistry Chemical Physics, 2019, 21, 14713-14721.	2.8	4
201	Utilization of Synergistic Effect of Dimensionâ€Differentiated Hierarchical Nanomaterials for Transparent and Flexible Wireless Communicational Elements. Advanced Materials Technologies, 2020, 5, 1901057.	5.8	4
202	Wearable Electronics: Wearable Electronics Based on 2D Materials for Human Physiological Information Detection (Small 15/2020). Small, 2020, 16, 2070083.	10.0	4
203	Enhancing the Ultraviolet Photocurrent and Response Speed of Zinc Oxide Nanoflowers using Surface Plasmons of Gold Nanoparticles and a Graphene Membrane. Physica Status Solidi - Rapid Research Letters, 2021, 15, 2000512.	2.4	4
204	Recent progress of continuous intraocular pressure monitoring. Nano Select, 2022, 3, 1-19.	3.7	4
205	A review on low-dimensional novel optoelectronic devices based on carbon nanotubes. AIP Advances, 2021, 11, .	1.3	4
206	A Flexible Graphene-Based Fabric Ultrasound Source for Machine Learning Enhanced Information Encryption. IEEE Electron Device Letters, 2022, 43, 1543-1546.	3.9	4
207	Withdrawal of "Fabrication and Properties of <formula formulatype="inline"> <tex notation="TeX">\$ hbox{Pt}/hbox{Bi}_{3.15}hbox{Nd}_{0.85}hbox{Ti}_{3}hbox{O}_{12}/hbox{HfO}_{2}/hbox{Si}\$</tex> </formula> Structure for Ferroelectric DRAM (FEDRAM) FET". IEEE Electron Device Letters, 2009, 30, 1111-1111.	3.9	3
208	A metrology of silicon film thermal conductivity using micro-Raman spectroscopy. , 2010, , .		3
209	A novel fatigue-insensitive self-referenced scheme for 1T1C FRAM. , 2010, , .		3
210	REACTION SIMULATION AND EXPERIMENT OF A Cl ₂ / Ar INDUCTIVELY COUPLED PLASMA FOR ETCHING OF SILICON. Surface Review and Letters, 2014, 21, 1450038.	1.1	3
211	Tailoring perpendicular magnetic anisotropy with graphene oxide membranes. RSC Advances, 2017, 7, 52938-52944.	3.6	3
212	High-Quality Reconfigurable Black Phosphorus p-n Junctions. IEEE Transactions on Electron Devices, 2018, , 1-5.	3.0	3
213	Ultrahigh Step-Up Coupled-Inductor DC-DC Converter With Soft-Switching for Driving Piezoelectric Actuators. IEEE Transactions on Circuits and Systems II: Express Briefs, 2021, 68, 2902-2906.	3.0	3
214	Fabricating In-Plane MoTe ₂ p-n Homojunction Photodetector Using Laser-Induced p-Type Doping. IEEE Transactions on Electron Devices, 2021, 68, 4485-4490.	3.0	3
215	Ambipolar transport compact models for two-dimensional materials based field-effect transistors. Tsinghua Science and Technology, 2021, 26, 574-591.	6.1	3

A multi-frequency wireless passive pressure sensor for TPMS applications. , 2009, , .

2

#	Article	IF	CITATIONS
217	Comparisons and analyses on heterostructures consisting of ZnO and different ferroelectric films. Materials Research Society Symposia Proceedings, 2011, 1368, 1.	0.1	2
218	PROTON IRRADIATION INFLUENCE ON THE MAGNETIC PROPERTIES OF GMR-SVs. Modern Physics Letters B, 2014, 28, 1450022.	1.9	2
219	A comparison of Pd and Au electrodes-based LiNbO ₃ surface acoustic wave devices. Modern Physics Letters B, 2016, 30, 1650349.	1.9	2
220	Simulation and experimental verification of silicon dioxide deposition by PECVD. Modern Physics Letters B, 2017, 31, 1750055.	1.9	2
221	Total-Ionizing-Dose Effects on a Graphene X-Ray Detector Laser-Scribed From Graphene Oxide. IEEE Transactions on Nuclear Science, 2018, 65, 473-477.	2.0	2
222	First Principles Study of Memory Selectors using Heterojunctions of 2D Layered Materials. , 2018, , .		2
223	Direct laser-patterned ultra-wideband antennae with carbon nanotubes. RSC Advances, 2018, 8, 31331-31336.	3.6	2
224	High sensitive surface-acoustic-wave optical sensor based on two-dimensional perovskite. , 2019, , .		2
225	Dualâ€Functional Nonvolatile and Volatile Memory in Resistively Switching Indium Tin Oxide/HfO <i>x</i> Devices. Physica Status Solidi (A) Applications and Materials Science, 2019, 216, 1900555.	1.8	2
226	Anomalous thermoacoustic effect in topological insulator for sound applications. Applied Physics Letters, 2020, 117, 123502.	3.3	2
227	Interfacial Regulation of Dielectric Properties in Ferroelectric Hf _{0.5} Zr _{0.5} O ₂ Thin Films. IEEE Journal of the Electron Devices Society, 2021, 9, 1093-1097.	2.1	2
228	Industrial-scale production of high-quality graphene sheets by millstone grinders. Journal Physics D: Applied Physics, 2022, 55, 164002.	2.8	2
229	Mini-review: Novel Graphene-based Acoustic Devices. Sensors and Actuators Reports, 2022, 4, 100086.	4.4	2
230	Exploration of the Mass Sensitivity of Quartz Crystal Microbalance under Overtone Modes Using Electrodeposition Method. Analytical Chemistry, 2022, 94, 5760-5768.	6.5	2
231	Modeling of Gate Tunable Synaptic Device for Neuromorphic Applications. Frontiers in Physics, 2021, 9,	2.1	2
232	Quasi-Fermi-Level Phase Space and its Applications in Ambipolar Two-Dimensional Field-Effect Transistors. Physical Review Applied, 2022, 17, .	3.8	2
233	Key Integration Techniques and Issues for Silicon-Based Ferroelectric Devices. Integrated Ferroelectrics, 2004, 66, 59-69.	0.7	1
234	Amplifier high linearization method based on offset cancellation technique. , 2009, , .		1

14

#	Article	IF	CITATIONS
235	Optimal RF IC design based on Fuzzy Genetic Algorithm. , 2009, , .		1
236	Implantable Subdural Electrode Arrays for Neural Recordings Based on MEMS Technologies. , 2009, , .		1
237	A novel method for fabricating 2-D array piezoelectric micromachined ultrasonic transducers for medical imaging. , 2009, , .		1
238	Study of Iridium Bottom Electrode in Ferroelectric Random Access Memory Application. Ferroelectrics, 2010, 406, 97-107.	0.6	1
239	A MEMS-based flexible electrode array using composite substrate. , 2010, , .		1
240	Micromachined piezoelectric devices for acoustic applications. , 2012, , .		1
241	Wafer-scale flexible graphene strain sensors. , 2013, , .		1
242	SIMULATION METHODS OF PIEZORESISTIVE PRESSURE SENSORS IN ORDER TO IMPROVE CONSISTENCY. Modern Physics Letters B, 2013, 27, 1350011.	1.9	1
243	An ultra-sensitive resistive pressure sensor based on the V-shaped foam-like structure of laser-scribed graphene. , 2014, , .		1
244	Large-scale fabrication of graphene-based electronic and MEMS devices. , 2014, , .		1
245	Modeling and analysis of nano-sized GMRs based on Co, NiFe and Ni materials. Science China Information Sciences, 2014, 57, 1-14.	4.3	1
246	A micro-scale microbial supercapacitor. , 2014, , .		1
247	Memory Devices: In Situ Tuning of Switching Window in a Gate-Controlled Bilayer Graphene-Electrode Resistive Memory Device (Adv. Mater. 47/2015). Advanced Materials, 2015, 27, 7766-7766.	21.0	1
248	A novel MEMS-based 13.56 MHz micro antenna for RFID application. , 2015, , .		1
249	Tunable and wearable high performance strain sensors based on laser patterned graphene flakes. , 2016, , .		1
250	An analytical charge-sheet drain current model for monolayer transition metal dichalcogenide negative capacitance field-effect transistors. , 2017, , .		1
251	A power manager system with 78% efficiency for high-voltage triboelectric nanogenerators. Science China Information Sciences, 2017, 60, 1.	4.3	1
252	Piezoelectric Micromachined Ultrasonic Transducers for Ultrasound Imaging. , 2018, , .		1

#	Article	IF	CITATIONS
253	High Performance and Wireless Graphene Earphone towards Practical Applications. , 2020, , .		1
254	Graphene muscle with artificial intelligence. , 2020, , .		1
255	The manufacture and characterization of a novel ultrasonic transducer for medical imaging. , 2021, , .		1
256	Self-Powered Multicolor Broadband Photodetector Based on GaSe/WSeâ,,//WSeâ,,/BP Van Der Waals Heterostructure. IEEE Transactions on Electron Devices, 2021, 68, 3881-3886.	3.0	1
257	Transistor Subthreshold Swing Lowered by 2-D Heterostructures. IEEE Transactions on Electron Devices, 2021, 68, 411-414.	3.0	1
258	Anisotropic electrical properties of aligned PtSe2 nanoribbon arrays grown by a pre-patterned selective selenization process. Nano Research, 0, , 1.	10.4	1
259	Biocompatible Sensors Are Revolutionizing Healthcare Technologies. , 2022, , 227-249.		1
260	Ultra-Low Voltage Schmitt Triggers Implemented by HfO ₂ -Based Ferroelectric Field-Effect Transistors. IEEE Electron Device Letters, 2022, 43, 1145-1148.	3.9	1
261	Cs ₂ AgBiBr ₆ -Tellurium heterojunction-based high-performance X-ray detectors. , 2022, , .		1
262	The α-In ₂ Se ₃ THz Photodetector. IEEE Transactions on Electron Devices, 2022, 69, 4371-4376.	3.0	1
263	Modeling and analysis of effect on bit-line voltage caused by imprint in FeRAM. , 2008, , .		0
264	OPTICAL CHARACTERIZATION OF Sr1â^'xBaxBi4Ti4O15 GRADED THIN FILMS. Integrated Ferroelectrics, 2008, 98, 128-135.	0.7	0
265	A novel circuit scheme and analysis for three-level feram. , 2008, , .		0
266	Buffer layer dependence of B <inf>3.15</inf> Nd <inf>0.85</inf> Ti <inf>3</inf> O <inf>12</inf> (BNdT) based MFIS capacitor for FeFET application. , 2008, , .		0
267	Comparison of PbZr1â^'xTixO3 thin films deposited on different substrates by liquid delivery metal organic chemical vapor deposition. Journal of Applied Physics, 2009, 105, 061611.	2.5	0
268	Bipolar switching analysis and negative resistance phenomenon in TiO. , 2010, , .		0
269	Nd-doped Bismuth Titanate based ferroelectric field effect transistor: Design, fabrication, and optimization. , 2011, , .		0
270	Research for piezoresistive pressure sensors: Methods to reduce the influence of processing deviation on sensitivity and improve product consistency. , 2011, , .		0

#	Article	IF	CITATIONS
271	ZnO nanorod array based optoelectronic device with graphene as transparent electrode. , 2012, , .		0
272	Multilayer graphene growth by a metal-catalyzed crystallization of diamond-like carbon. , 2012, , .		0
273	Light-Induced Modulation in Resistance Switching of Carbon Nanotube/ BiFeO ₃ /Pt Heterostructure. Integrated Ferroelectrics, 2012, 132, 53-60.	0.7	0
274	Novel flexible nanogenerators. , 2014, , .		0
275	Graphem stack: Growth, characterization and diverse devices. , 2015, , .		0
276	Biological information wireless monitoring system. , 2015, , .		0
277	A universal method to grow and etch graphene film. , 2016, , .		0
278	Novel memory devices based on nanostructured carbon materials. , 2016, , .		0
279	A common-source amplifier based on single layer MoS <inf>2</inf> . , 2016, , .		0
280	Novel graphene-based resistive random access memory. , 2016, , .		0
281	Electrical thermal acoustic point source based on mems technology. , 2016, , .		0
282	Novel Field Effect Transistor Fabrication Based on Non-Graphene 2D Materials. MRS Advances, 2017, 2, 3675-3684.	0.9	0
283	A simple way to grow large-area single-layer MoS <inf>2</inf> film by chemical vapor deposition. , 2017, , .		Ο
284	A Two-terminal Electric-double-layer Synaptic Device with Short-term Plasticity. , 2018, , .		0
285	Miniaturized and High Precision Monitoring System for Natural Waters Using a Microflow Analyzer. , 2019, , .		Ο
286	Graphene-based Wearable Sensors for Physiological Signal Monitoring. , 2019, , .		0
287	Scalable Modeling for the Coplanar Waveguide Step Discontinuity at Frequency up to 150 GHz. , 2019, , .		0
288	Introductory Chapter: Perovskite Materials and Advanced Applications. , 0, , .		0

#	Article	IF	CITATIONS
289	A Spectrum-Tunable and Flexible Light-Emitting Device with Ultra-Wide Wavelength Range. , 2020, , .		0
290	Thermal Energy Conversion: Grapheneâ€Based Devices for Thermal Energy Conversion and Utilization (Adv. Funct. Mater. 8/2020). Advanced Functional Materials, 2020, 30, 2070052.	14.9	0
291	Stability diagrams of two optically mutual-injected quantum cascade lasers. AIP Advances, 2021, 11, 015320.	1.3	0
292	Flexible and Transparent Ultraviolet Photodetector Enabled by Metal Doping ZnO Nanorods Based on Mica Substrate. , 2021, , .		0
293	A Sensitive Vertical Standing Graphene/Silicon Schottky Photodetector to Angle Changes. , 2021, , .		0
294	Large Coercive Field in Hf0.5Zr0.5O2-based Capacitors with Gd Top Electrode. , 2021, , .		0
295	Progress of Lead-Free Halide Perovskite X-ray Detectors. , 2020, , .		0
296	A Low-cost, Low-power, and Practical Nano-heterojunction Pollution Gas Sensor Based on Accurate Dielectrophoresis Technology. , 2022, , .		0
297	Investigation of Q Factor of the QCM Resonator Under Overtone Modes. , 2022, , .		0